Cellular/Molecular

Na^+, Cl^-, and pH Dependence of the Human Choline Transporter (hCHT) in *Xenopus* Oocytes: The Proton Inactivation Hypothesis of hCHT in Synaptic Vesicles

Hideki Iwamoto, Randy D. Blakely, and Louis J. De Felice
Department of Pharmacology and Center for Molecular Neuroscience, Vanderbilt University School of Medicine, Nashville Tennessee 37232-8548

The recent cloning of the human choline transporter (hCHT) has allowed its expression in *Xenopus laevis* oocytes and the simultaneous measurement of choline transport and choline-induced current under voltage clamp. hCHT currents and choline transport are evident in cRNA-injected oocytes and significantly enhanced by the hCHT trafficking mutant L530A/V531A. The charge/choline ratio of hCHT varies from 10*e*/choline at −80 mV to 3*e*/choline at −20 mV, in contrast with the reported fixed stoichiometry of the Na^+-coupled glucose transporter in the same gene family. Ion substitution shows that the choline uptake and choline-induced current are Na^+ and Cl^- dependent; however, the reversal potential of the induced current suggests a Na^+-selective mechanism, consigning Cl^- to a regulatory role rather than a coupled, cotransported-ion role. The hCHT-specific inhibitor hemicholinium-3 (HC-3) blocks choline uptake and choline-induced current; in addition, HC-3 alone reveals a constitutive, depolarizing leak current through hCHT. We show that external protons reduce hCHT current, transport, and binding with a similar pKa of 7.4, suggesting proton titration of residue(s) that support choline binding and transport. Given the localization of the choline transporter to synaptic vesicles, we propose that proton inactivation of hCHT prevents acetylcholine and proton leakage from the acidic interior of cholinergic synaptic vesicles. This mechanism would allow cholinergic, activity-triggered delivery of silent choline transporters to the plasma membrane, in which normal pH would reactivate the transporters for choline uptake and subsequent acetylcholine synthesis.

Key words: **choline transporter; *Xenopus* oocyte; choline-induced current; Na^+; Cl^-; pH**

Introduction

Cholinergic neurons release acetylcholine (ACh) for autonomic functions in sympathetic and parasympathetic neurons as well as cognitive activity associated with central pathways (Dani and DeBiasi, 2001; Bymaster et al., 2003). After ACh hydrolysis by acetylcholinesterase, the plasma membrane choline transporter (CHT) returns choline to the presynaptic terminal for ACh synthesis (Kuhar and Murrin, 1978; Okuda and Haga, 2003; Ferguson and Blakely, 2004; Sarter and Parikh, 2005; Ribeiro et al., 2006), and vesicular acetylcholine transporters (VAChT) package ACh in synaptic vesicles (Parsons et al., 1993; Eiden, 1998). High-affinity (K_m of 1–2 μM) CHTs are distinguished from low-affinity choline transporters by Na^+ and Cl^- dependence and hemicholinium-3 (HC-3) [inhibition constant (K_i) of 5 nM] block (Yamamura and Snyder, 1972; Guyenet et al., 1973; Haga and Noda, 1973). Abnormal regulation of CHT contributes to cognitive impairments and neuropsychiatric disorders, including Alzheimer's disease (Ferguson and Blakely, 2004; Sarter and Parikh, 2005; Bales et al., 2006), emphasizing the need to understand CHT regulation.

Cholinergic neurons increase choline uptake via CHT in proportion to ACh demand and resynthesis (Simon and Kuhar, 1975; Collier et al., 1983; Lowenstein and Coyle, 1986). Ferguson et al. (2003) show that CHT is concentrated at central and peripheral cholinergic terminals, in which they are localized in presynaptic vesicles that store ACh via VAChTs. Furthermore, cholinergic activity increases CHT density on the plasma membrane, implying that vesicles in cholinergic terminals deliver CHTs to the membrane, coupling ACh release to choline transport. VAChT concentrates ACh inside vesicles using the proton gradient across the vesicle membrane (Parsons et al., 1993; Eiden, 1998); however, CHT is permeable to ACh at high concentrations (Marchbanks and Wonnacott, 1979) and is positioned to transport ACh out of vesicles. Although CHT is an Na^+-coupled transport system, studies of the homologous Na^+–glucose transporter (SGLT1) demonstrate a capacity to drive transport using a pH gradient (Hirayama et al., 1994). Thus, whereas CHT is located on ACh-containing vesicles for delivery to the plasma membrane in proportion to demands for choline reuptake, it could work against ACh and proton concentration if it were functional in this compartment.

The low density of CHT in mammalian cholinergic neurons

Received May 2, 2006; revised Aug. 11, 2006; accepted Aug. 11, 2006.

This work was supported by National Institutes of Health Grants MH-73159 (R.D.B.) and NS-34075 (L.J.D.F.) and an Alzheimer's Association Zenith Award (R.D.B.). We gratefully acknowledge Dr. Alicia Ruggiero for providing us with the hCHT LV mutant and assistance with the biotinylation studies. We also thank Hongping Yuan for plasmid preparations and Drs. Keith Henry, Maureen Hahn, Dawn Matthies, Chongbin Zhu, and Uhna Sung, Katrina Brewer, and Prof. Yuanmou Liu for their help with this project.

Correspondence should be addressed to Dr. Louis J. De Felice, Department of Pharmacology, Center for Molecular Neuroscience, 7130 Medical Research Building III, Vanderbilt University Medical Center, 465 21st Avenue South, Nashville, TN 37232-8548. E-mail: lou.defelice@vanderbilt.edu.

DOI:10.1523/JNEUROSCI.1862-06.2006

 0270-6474/06/269851-09$15.00/0

hampered efforts to clone and characterize CHT. However, the cloning of CHT cDNA (*cho-1*) from *Caenorhabtiditis elegans* (Okuda et al., 2000) led to mammalian orthologs from rat (Okuda et al., 2000), mouse (Apparsundaram et al., 2001), and human (Apparsundaram et al., 2000; Okuda and Haga, 2000). Phylogenetic analysis demonstrates that CHT belongs to the Na^+/glucose cotransporter family (SLC5), although at present CHT is the only member identified with neurotransmission (Ferguson and Blakely, 2004; Wright and Turk, 2004). Here we report the expression of the human choline transporter (hCHT) in *Xenopus leavis* oocytes, a paradigm that allows a thorough biophysical analysis of choline uptake and choline-induced current, using the two-electrode voltage-clamp technique. Our data provide a mechanistic basis for inactivation of CHT in ACh vesicles, rendering CHT nonfunctional in vesicles, and the re-activation of CHT once delivered to the plasma membrane, in which its presence is crucial to acetylcholine synthesis.

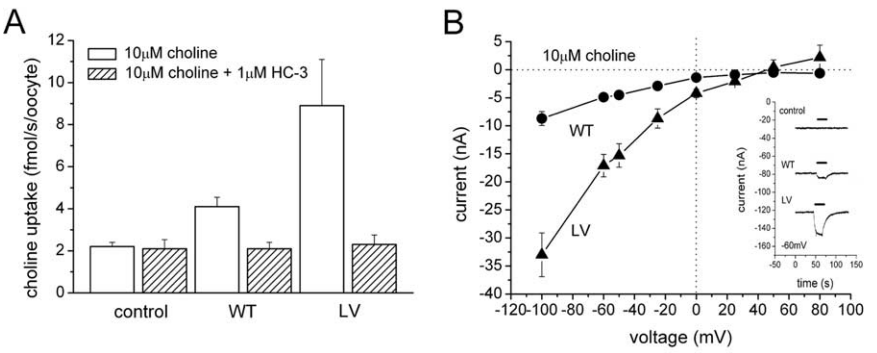

Figure 1. Choline uptake and choline-induced current in hCHT-expressing oocytes. ***A***, Uptake assays were performed with 10 μM choline containing 1% [^{3}H]choline and measured over a period of 30 min in both hCHT WT-expressing and LV-expressing oocytes with and without 10 min preincubation of the hCHT-specific inhibitor HC-3 at 1 μM ($n = 5–8$). ***B***, The choline-induced *I–V* curves were generated by brief exposure to 10 μM choline at various membrane potentials ($n = 5$). Baseline current in the absence of choline was subtracted from the choline-induced current. Inset, Choline at 10 μM induced a significant current when the oocyte was held at −60 mV. Note that the holding currents in WT- and LV-expressing oocyte are shifted compared with control oocyte.

Materials and Methods

hCHT expression in Xenopus leavis *oocytes.* The isolation of oocytes and cRNA preparation were described previously (Ramsey and DeFelice, 2002; Adams and DeFelice, 2003). Briefly, stage V–VI oocytes were harvested from *Xenopus laevis* (Nasco, Modesto, CA). After harvest, the follicle cell layer was removed by incubation with 2 mg/ml collagenase in Ringer's buffer (in mM: 96 NaCl, 2 KCl, 5 $MgCl_2$, and 5 HEPES, pH 7.4) for 1 h. cRNA injections were performed on the day of harvest. hCHT wild-type (WT) (Apparsundaram et al., 2000) and hCHT L530A/V531A (LV) (A. M. Ruggiero, S. M. Ferguson, and R. D. Blakely, unpublished observations) cRNA were transcribed from *Not*I (New England Biolabs, Beverly, MA)-digested cDNA in pOTV vector (a gift of Dr. Mark Sonders, Columbia University, New York, NY) using Ambion (Austin, TX) mMessage Machine T7 kit. hCHT is constitutively internalized from the plasma membrane, an important mechanism for activity-dependent trafficking of hCHT. In searching for trafficking motifs in the hCHT C terminal, A. M. Ruggiero, S. M. Ferguson, and R. D. Blakely (unpublished observations) identified a di-leucine trafficking motif of hCHT and demonstrated that the LV mutant slows internalization. The di-leucine motif is thought to be an interaction site with adaptor proteins that mediate clathrin-dependent internalization. Recently, Ribeiro et al. (2005) identified the same motif in rat CHT, and it has also been found in VAChT (Tan et al., 1998) and is speculated to be a common sorting signal for endocytic vesicle targeting (Ferguson and Blakely, 2004). During the course of our experiments, it was discovered that the LV mutant we were using actually contained an additional mutation, L538V; however, L530A/V531A/L538V is functionally identical to L530A/V531A (unpublished uptake and electrophysiological data from A. Ruggiero and H. Iwamoto), and thus we have retained the simpler notation, LV. The cRNA concentrations were confirmed by UV spectroscopy and gel electrophoresis. Each oocyte was injected with 23 ng of cRNA and incubated at 18°C for 4–6 d in Ringer's buffer supplemented with 550 μM/ml sodium pyruvate, 100 μg/ml streptomycin, 50 μg/ml tetracycline, and 5% dialyzed horse serum. Healthy oocytes were selected by visual inspection for subsequent electrophysiological and biochemical assays.

Two-electrode voltage clamp. Whole-cell currents were measured with two-electrode voltage-clamp techniques using a GeneClamp 500 (Molecular Devices, Palo Alto, CA). Microelectrodes were pulled using a programmable puller (model P-87; Sutter Instruments, Novato, CA) and filled with 3 M KCl (0.5–3 MΩ resistance). A 16-bit analog-to-digital converter (Digidata 1322A; Molecular Devices) interfaced to a personal computer (PC) running Clampex 9 software (Molecular Devices) was used to control membrane voltage and to acquire data. To induce hCHT-associated current, oocytes were perfused with choline chloride dissolved in modified Ringer's solution (in mM: 100 NaCl, 5 potassium gluconate, 5 HEPES, 1 $MgSO_4$, and 0.5 calcium acetate, pH 7.4) using a gravity-flow system (4–5 ml/min flow rate). pH of buffer was adjusted with *N*-methyl-D-glucamine or phosphoric acid. To minimize liquid junction potentials, chloride substitution experiments were performed using a salt bridge to isolate the Ag–AgCl electrode from the bath. For constant-voltage recordings, data were low-pass filtered at 10 Hz and digitized at 20 Hz. For current–voltage (*I–V*) recordings, the voltage was changed stepwise every 500 ms. Currents were low-pass filtered at 100 Hz and digitized at 200 Hz. All analyses were performed using Origin 7 (Microcal, Northampton, MA).

Surface-biotinylation Western blotting. The full procedures were described previously (Ramsey and DeFelice, 2002). Briefly, equal numbers of oocytes from each cRNA injection (typically 20) were incubated with 1 mg/ml EZ-Link Sulfo-NHS-SS-Biotin (Pierce, Rockford, IL) in ice-cold PBS solution. After terminating the biotinylation with ice-cold PBS containing 100 mM glycine, the oocytes were solubilized with lysis buffer (150 mM NaCl, 10 mM Tris, 1 mM EDTA, 1% Triton X-100, 0.1% SDS, 250 μM phenylmethylsulfonyl fluoride (PMSF), 1 μM pepstatin, 1 μg/ml leupeptin, and 1 μg/ml aprotinin). The supernatant was separated from insoluble yolk materials by centrifugation, and the protein concentration was determined using the bicinchoninic acid (BCA) regent (BCA protein assay kit; Pierce). To obtain surface-biotinylated proteins, the supernatant was incubated with streptavidin beads (Pierce) for 45 min at room temperature. Biotinylated proteins were subjected to SDS-PAGE in a 10% polyacrylamide gel, and blots were transferred to polyvinylidene difluoride membranes (NEN, Boston, MA). Blots were incubated with rabbit polyclonal anti-hCHT antibody (1:1000 dilutions) (Ferguson et al., 2003). After extensive washing, blots were incubated with horseradish peroxidase-conjugated goat anti-rabbit antibody (Jackson ImmunoResearch, West Grove, PA). The immunoreactive proteins were detected using Western Lightning Chemiluminescence Regent Plus (PerkinElmer, Boston, MA) and Hyperfilm ECL (Amersham Biosciences, Buckinghamshire, UK). Multiple exposures were obtained to ensure quantification in the linear range of the film. Band densities were quantified with Scion (Frederick, MD) Image software (PC version of NIH Image).

[^{3}H]Choline transport assays. Choline uptake in WT- or LV-expressing oocytes was measured by incubation with 10 μM choline chloride containing 1% of [^{3}H]choline chloride (86 Ci/mmol; PerkinElmer) in modified Ringer's buffer for 30 min at room temperature. Assays were terminated by washing extensively with ice-cold buffer. Specific uptake was defined by subtracting the uptake obtained in nontransfected, water-injected control oocytes from uptake in cRNA-injected oocytes. Oocytes

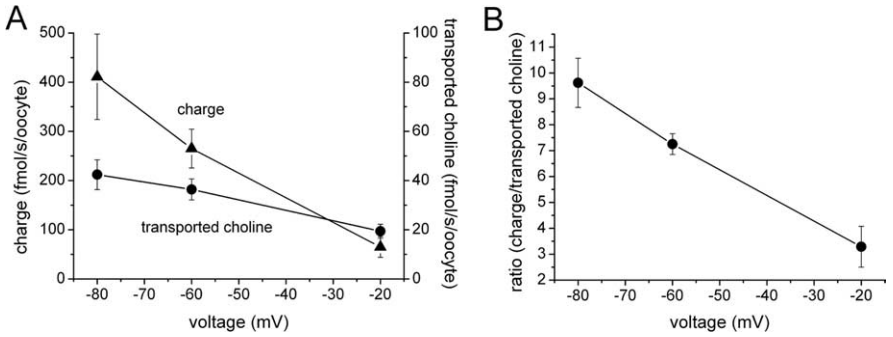

Figure 2. Simultaneous measurement of uptake and current. ***A***, Choline at 10 μM containing 1% [^{3}H]choline induced current and promoted choline uptake, which were measured concurrently in the same oocyte under voltage clamp for 500 s (for details, see Materials and Methods). Each point consists of data from three to four different oocytes. The LV mutant was used in this experiment. ***B***, The charge/substrate ratio is plotted as a function of voltage from the data in *A*.

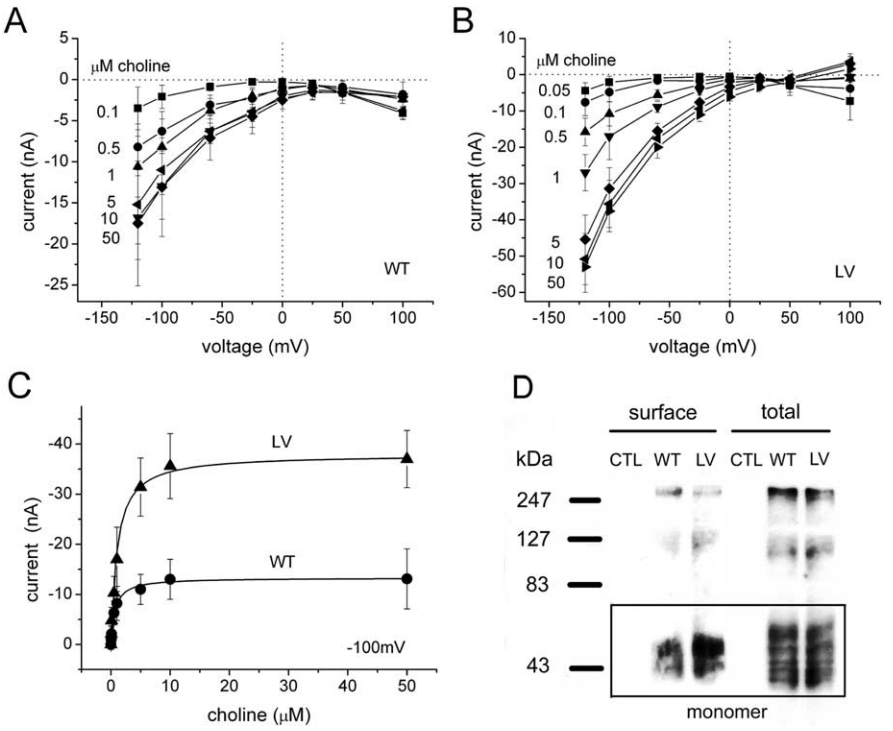

Figure 3. The *I–V* curves for WT and LV transporters for various choline concentrations. *I–V* curves measured with choline concentrations from 0.05 to 50 μM for WT (***A***) and the LV mutant (***B***) ($n = 5$). ***C***, From ***A*** and ***B***, the currents at -100 mV are plotted for different choline concentrations. These data were then fit to a Michaelis–Menten equation to obtain the apparent affinity (K_m) and maximal current (I_{max}). K_m of 0.7 ± 0.1 μM and I_{max} of -13.3 ± 0.2 nA for WT. K_m of 1.0 ± 0.1 μM and I_{max} of -37.9 ± 0.3 nA for LV. ***D***, Surface biotinylation Western blotting. Water-injected control oocytes show no detectable hCHT expression (CTL). A rectangular box represents hCHT monomers. Band densities of surface fraction at 55 kDa show that LV is 2.6 ± 0.3 times greater than WT ($n = 3$), consistent with I_{max} differences between LV and WT. Total expression for WT and LV show no significant differences (Student's *t* test, $p > 0.05$; $n = 3$).

were solubilized with 1% SDS, and choline accumulation was quantified with a liquid scintillation counter (TopCount NXT; Packard Instrument Company, Meriden, CT).

[^{3}H]Hemicholinium-3 binding assays. Most procedures were the same as those used for choline uptake experiments described above. The WT- or LV-expressing oocytes were incubated with 10 nM [^{3}H]HC-3 (125 Ci/mmol; PerkinElmer) in modified Ringer's solution for 30 min at room temperature (Sandberg and Coyle, 1985; Ferguson et al., 2004). To obtain sufficient binding signal, two oocytes were placed in each well. Binding assays were terminated by washing extensively with the ice-cold buffer. Specific binding was defined by subtracting the binding obtained to nontransfected, water-injected oocytes from binding to cRNA-injected oocytes.

Simultaneous measurement of choline uptake and choline-induced current. Simultaneous measurement of choline uptake and choline-induced current was performed under voltage-clamp conditions, using techniques described previously (Petersen and DeFelice, 1999; Loo et al., 2000; Ramsey and DeFelice, 2002; Quick, 2003). Oocytes were perfused for 500 s under voltage clamp with 10 μM choline containing 1% [^{3}H]choline. Uptake was terminated by extensive perfusion with buffer. To minimize loss of choline, the oocyte was perfused with ice-cold buffer before removing the oocytes from the chamber. The total charge was calculated by time integration of choline-induced inward current and correlated with uptake in the same oocyte. Nonspecific uptake was determined with water-injected control oocytes under the same condition.

Results

Choline induces an inward current in hCHT-expressing oocytes

Oocytes expressing the hCHT WT take up [^{3}H]choline (Fig. 1*A*) and generate inward currents when choline is added to the bath (Fig. 1*B*). In mammalian cells, the trafficking mutant LV results in increased surface expression (Ruggiero, Ferguson, and Blakely, unpublished observation). In oocytes, the choline uptake and choline-induced current in LV mutants are approximately three times larger than WT uptake and currents under the same conditions (Fig. 1*A*,*B*). In addition, WT and LV oocytes have shifted holding currents for the same voltage, indicating a constitutive depolarization in the absence of choline (leak current) (Fig. 1*B*, inset). Water-injected oocytes show no detectable choline-induced current. Figure 1*B* plots the relationship between choline-induced current (bars in inset) and membrane voltage. The *I–V* curves for WT have no detectable reversal potential, whereas LV reversal potentials are in the range of 45–60 mV. The reversal potential for LV is near the Nernst potential for Na^+, 39 mV at room temperature, if we assume that internal Na^+ concentration in oocytes is 22 mM (Kusano et al., 1982).

hCHT charge/choline ratio depends on voltage

Choline-induced currents in hCHT oocytes suggest that choline transport is electrogenic, i.e., net charge accompanies choline flux. To examine how many charges attend each choline molecule during transport, we measured choline uptake and choline-induced current simultaneously under voltage clamp. Figure 2*A* shows that choline uptake depends on membrane voltage. Although charge and uptake both decrease with depolarization, the charge/flux ratio is not constant. Figure 2*B* shows that the charge/choline ratio varies linearly from ~10 at -80 mV to 3 at -20 mV.

LV has increased surface expression, which correlates with transport and current

The choline-induced hCHT current in WT and LV depends on not only voltage but also on choline concentration (Fig. 3*A*,*B*). To obtain the apparent affinity (K_m) of choline for hCHT, we plotted the current at −100 mV against the choline concentration (Fig. 3*C*). Fitting these data to a single-binding-site model, the K_m is similar for both WT and the LV mutant (0.7 ± 0.1 and 1.0 ± 0.1 μM, respectively; $n = 5$). The K_m obtained from choline-induced current is comparable with that for choline uptake in *Xenopus* oocytes and mammalian cells (Apparsundaram et al., 2000; Okuda and Haga, 2000; Okuda and Haga, 2003; Ferguson and Blakely, 2004). For WT, maximal current (I_{max}) at −100 mV was -13.3 ± 0.15 nA, and, for the LV, I_{max} was -37.9 ± 0.30 nA. The difference in I_{max} between WT and LV is explained by the differences in surface expression for these transporters. Surface biotinylation shows that, for the same cRNA injection, LV expresses 2.6 ± 0.3 times more surface protein than WT ($n = 3$) (Fig. 3*D*). The total expression level of WT and LV shows no significant difference (Student's *t* test, $p > 0.05$; $n = 3$).

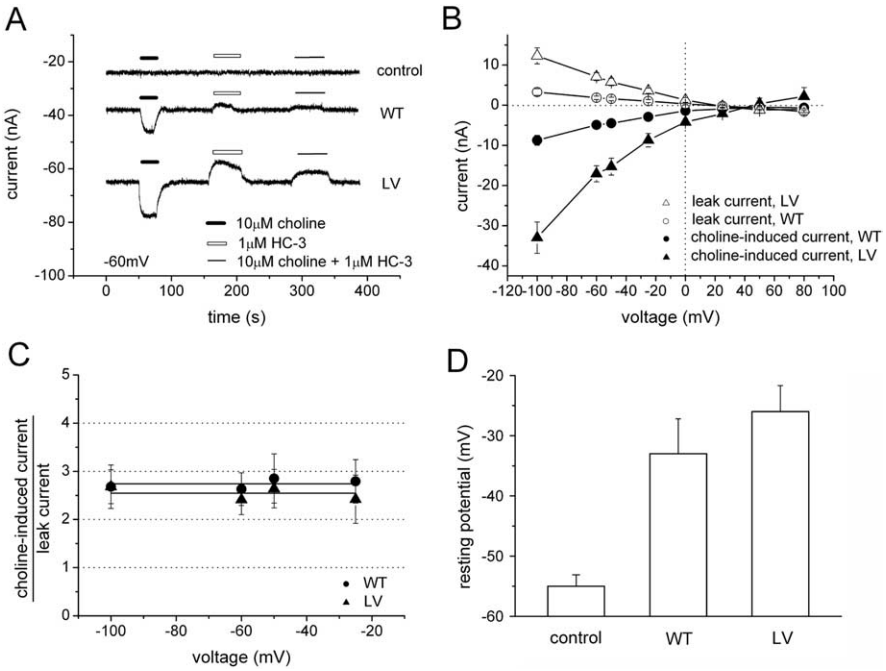

Figure 4. HC-3 inhibits choline-induced current. ***A***, HC-3 at 1 μM inhibits the choline-induced current (10 μM choline at −60 mV). Perfusion of 1 μM HC-3 alone reveals an apparent outward current (leak) in the transporter (white bar). There was no detectable leak current for control oocytes under the same conditions. A slow baseline drift was removed from ***A***. ***B***, *I–V* curves for 10 μM choline-induced current and 1 μM HC-3-revealed leak current were obtained from WT and LV mutants ($n = 5$). ***C***, The ratio of choline-induced current to HC-3-revealed leak current is calculated from ***B***. The ratio is constant at any voltage for either WT or LV. ***D***, Leak current depolarizes oocytes. Resting potentials were assessed in water-injected control oocytes, WT-expressing oocytes, and LV-expressing oocytes in the absence of choline. Compared with the water-injected control oocytes, resting potentials in WT- and LV-expressing oocytes were significantly depolarized ($n = 7$).

HC-3 reveals leak current in the absence of choline

HC-3 is a potent and specific inhibitor for high-affinity choline uptake (K_i of 5 nM) (Okuda and Haga, 2003; Ferguson and Blakely, 2004) (Fig. 1*A*). Perfusion with HC-3 alone reveals a leak current in choline-competent cells (upward deflection), which is interpreted as HC-3 block of an endogenous hCHT leak current. HC-3 blocks virtually all induced current in both WT and LV (Fig. 4*A*), and leak current and choline-induced current reversal potentials are identical within experimental error (45–60 mV) (Fig. 4*B*) and close to the theoretical Nernst potential for Na^+ (39 mV). These data imply that both the leak and the induced currents are carried predominately by Na^+ ions; however, the possibility of other ions, including protons, cannot be excluded. Additionally, HC-3 blocks the leak and induced current to the same degree, further implying a common pathway. Both leak currents and induced currents are voltage dependent (Fig. 4*B*), but their ratio is the same for either WT or LV (Fig. 4*C*), which indicates that the molecular properties of leak are not altered for WT and LV. Other transporters, such as the SGLT1 (Hirayama et al., 1994; Mackenzie et al., 1998) in the same family, as well as serotonin transporter (SERT) (Mager et al., 1994; Galli et al., 1997; Petersen and DeFelice, 1999; Adams and DeFelice, 2003) and norepinephrine transporter (NET) (Galli et al., 1995), also exhibit leak currents proportional to induced currents. In the absence of choline, the resting potentials of WT- or LV-expressing oocytes are depolarized compared with water-injected controls (Fig. 4*D*). Oocytes expressing LV mutants are consistently more depolarized than oocytes expressing WT, in agreement with the holding current shifts (Fig. 1*B*, inset).

Choline-induced currents depend on external Na^+ and Cl^-

Na^+ and Cl^- are necessary for high-affinity choline uptake (Simon and Kuhar, 1976; Kuhar and Murrin, 1978; Okuda and Haga, 2000). Furthermore, choline-induced currents depend on these ions. To study cations, we replaced NaCl with equimolar KCl, LiCl, or tetraethylammonium-Cl (TEACl). Because of greater similarity of measurements with higher levels of CHT surface expression, we present data from LV-expressing oocytes (data from WT not shown). In water-injected controls, these substitutions result in substantial baseline shifts, especially KCl and TEA solutions; however, no choline-induced currents occur in any solution (Fig. 5*A*). In LV-expressing oocytes, choline-induced currents occur only in NaCl solutions (Fig. 5*B*). The baseline shifts in LV-expressing oocytes differ from controls, especially for KCl and TEA substitutions. These differences are likely explained by lower resting potentials in LV oocytes (Fig. 4*D*). No Li-induced leak was found in LV oocytes, in contrast to other Na^+-coupled neurotransmitter transporters (Mager et al., 1996; Galli et al., 1997; Petersen and DeFelice, 1999; Adams and DeFelice, 2003; Karakossian et al., 2005). For anion substitutions, NaCl was replaced with NaBr, Na gluconate (NaGlu), or Na sodium methanesulfonate (NaMS). Control oocytes elicit no choline-induced current for these anions (data not shown). Choline-induced currents occur only in NaCl and NaBr (Fig. 5*C*). However, the current, although not eliminated in NaBr, was only ~30% of that in NaCl. Figure 5*D* summarizes the external anion and cation dependence of choline-induced current in WT- and LV-expressing oocytes. These data show that choline-induced hCHT current depends on both Na^+ and Cl^-. No difference in ion dependence was found between WT and LV oocytes.

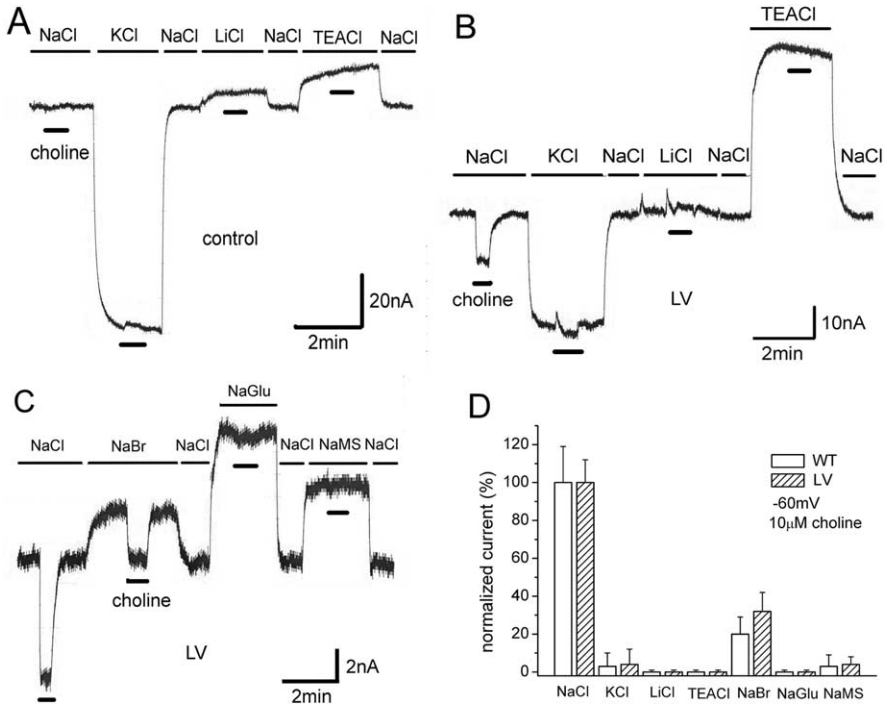

Figure 5. The role of cations and anions in the choline-induced current. ***A***, The effect of cation substitutions in control oocytes. NaCl at 100 mM was replaced with equimolar KCl, LiCl, or TEACl. No choline-induced current was observed when 10 μM choline (thick black bars) was perfused onto water-injected control oocytes held at −60 mV. The baseline is normalized to the value in NaCl. ***B***, Effect of cation substitutions in LV oocytes. Choline-induced current is observed only in NaCl. The magnitude of baseline shift with cation substitution is different LV oocytes compared with control oocytes. ***C***, Effect of anion substitutions in LV-expressing oocytes. NaCl at 100 mM was replaced with equimolar NaBr, NaGlu, or NaMS. Choline-induced current was observed only in NaCl and NaBr. No choline-induced current was observed in water-injected control oocytes. The magnitude of baseline shift with anion substitution is different LV oocytes compared with control oocytes (data not shown). ***D***, Summary of cation and anion dependence of choline-induced current ($n = 5$). Choline-induced current depends strictly on Na^+ but less stringently on Cl^-, because Br^- can partially replace Cl^-. Essentially no difference exists in ionic dependence between WT and LV hCHT-expressing oocytes.

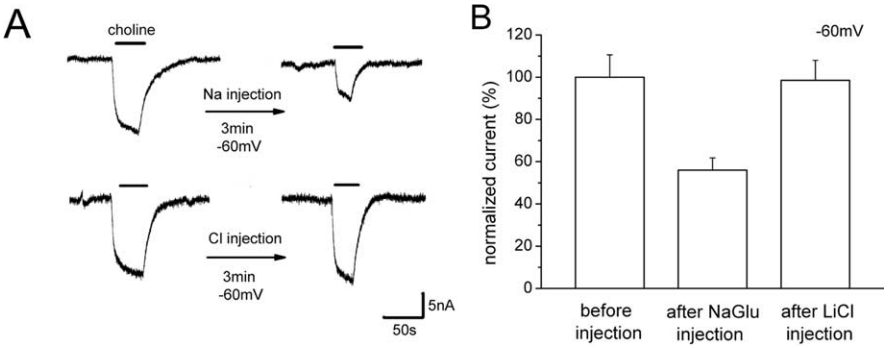

Figure 6. Internal Na^+, but not Cl^-, suppresses the choline-induced current. ***A***, Top row, NaGlu (46 nl of 0.5 M) was injected into LV-expressing oocytes. The final concentration of internal NaGlu is ~23 mM NaGlu in oocytes, assuming a volume of 1 μl. The figure shows typical data in 10 μM choline before and 3 min after the injection, in oocytes held at −60 mV. ***A***, Bottom row, LiCl (46 nl of 0.5 M) was injected into an LV-expressing oocyte. The final concentration of LiCl inside is ~23 mM. Similar to ***A***, the 10 μM choline-induced current was monitored at −60 mV before and 3 min after the injection. ***B***, Summary. The effect of NaGlu and LiCl injections on choline-induced current. The currents are normalized to the current before injection (100 ± 10.6%; $n = 4$). Internal NaGlu reduced the induced current by 50% 3–5 min after the injection (56.0 ± 5.8%; $n = 4$). However, internal LiCl had almost no effect on the induced current (98.5 ± 9.5%; $n = 4$).

Internal Na^+ reduces choline-induced current, but Cl^- has no similar effect

The reversal potential of choline-induced current suggests that hCHT is Na^+ selective (Fig. 1*B*); however, the induced current requires both external Na^+ and Cl^- (Fig. 5*D*). This is explained if hCHT uses external Cl^- to regulate transport but does not transport Cl^-. To test this idea, LiCl was injected into oocytes, which should inhibit the induced current if it is partly carried by Cl^-. To test this expectation for Na^+, we injected NaGlu into the oocyte. When a high concentration of NaGlu was injected (final concentration is ~23 mM NaGlu added to the inside the oocyte), the choline-induced current showed an ~50% reduction (Fig. 6*A*, top row). However, in the same protocol, the choline-induced current was insensitive to internal LiCl (final concentration of 23 mM LiCl added to the inside the oocyte) (Fig. 6*A*, bottom row). Figure 6*B* summarizes the effect of NaGlu and LiCl injection on choline-induced current, indicating that Cl^- plays a different role than Na^+ and is likely a regulatory ion rather than cotransported ion.

pH regulates choline-induced current, choline transport, and HC-3 binding

We found that choline-induced current depends not only on Na^+ and Cl^- but also on external pH. Figure 7*A* shows pH dependence of 10 μM choline-induced current at −60 mV. The current is abolished at pH 5.5. The activation and deactivation of choline-induced currents by pH is reversible (data not shown). Figure 7*B* shows the normalized pH dependence of choline-induced current, indicating a pKa of 7.4. No significant difference between WT and LV was observed. We measured *I–V* curves for 10 μM choline-induced currents for pH between 5.5 and 8.5. The currents at different pH intersect over a narrow range of voltages (30–50 mV) (supplemental figure, available at www.jneurosci.org as supplemental material), which appears to be independent of pH. However, because the induced current is small near reversal and smaller still at low pH, it is difficult to determine relative ionic permeation from reversal potentials. Choline uptake (Fig. 7*C*) and HC-3-specific binding (Fig. 7*D*) exhibit similar pH dependences. One concern is that the pKa is close to that of HEPES buffer (pKa of 7.55), and HEPES has structural similarity to choline (both have an *N*-ethylalcohol moiety). Thus, the possibility exists that HEPES could cause pH-dependent inhibition of hCHT current (Ming et al., 2002). However, structurally dissimilar buffers Tris [Tris(hydroxymethyl)aminomethane] and MOPS [3-(*N*-morpholino) propanesulfonic acid] gave similar pH dependence (data not shown). Another consideration is the deprotonation of choline; however, choline has pKa of 13.9 (Perrin, 1972). Therefore, the charge on choline is constant in our experimental pH range. The pH dependence of cho-

line-induced current is therefore most likely a titration of a functional group on the hCHT protein itself. It may be interesting to note that, as a quaternary ammonium, choline does not alter its charge after entering the vesicle. Other neurotransmitters, such as GABA, 5-HT, norepinephrine, and dopamine (DA), are only partially charged in the cytosol but fully charged in the acidic vesicle.

Na^+ and Cl^- dependence of the choline-induced current at different pH

To further investigate possible pH mechanisms, we measured the effect of protons on choline-induced current under different ionic conditions. Figure 8*A* shows the effect of pH on the induced current as a function of choline concentration. Whereas the apparent affinity for choline changes only weakly with pH, I_{max} changes dramatically. Furthermore, I_{max} changes in <30 s (limited by the solution exchange), which is too fast for insertion of transporters into the membrane. This is consistent with biotinylation data, which reveal no change in transporter surface expression at any pH (data not shown), suggesting that pH affects the catalytic activity of individual transporters already in the membrane. Figure 8, *B* and *C*, shows the Na^+ and Cl^- concentration dependence of the choline-induced current at different pH. Striking differences are evident: whereas the choline-induced current depends linearly on Na^+ at concentrations <100 mM (Fig. 8*B*), Cl^- dependence saturates in this range (Fig. 8*C*), with half-maximal Cl^- concentration in the range of 15–35 mM. Figure 8*D* summarizes the pH-dependent currents for Na^+ and Cl^- on normalized scales, showing that Na^+ or Cl^- stimulation of the choline-induced current has the same concentration dependence at any pH. Furthermore, the Na^+ and Cl^- dependences for induced current are similar to Na^+ and Cl^- dependences for HC-3-specific binding (Fig. 8*E*,*F*). Thus, protons change I_{max} of choline-induced current but not K_m for choline. Similarly, protons change the magnitude of choline-induced current and HC-3 binding titrated against Na^+ or Cl^- ions but not the shape of the curves.

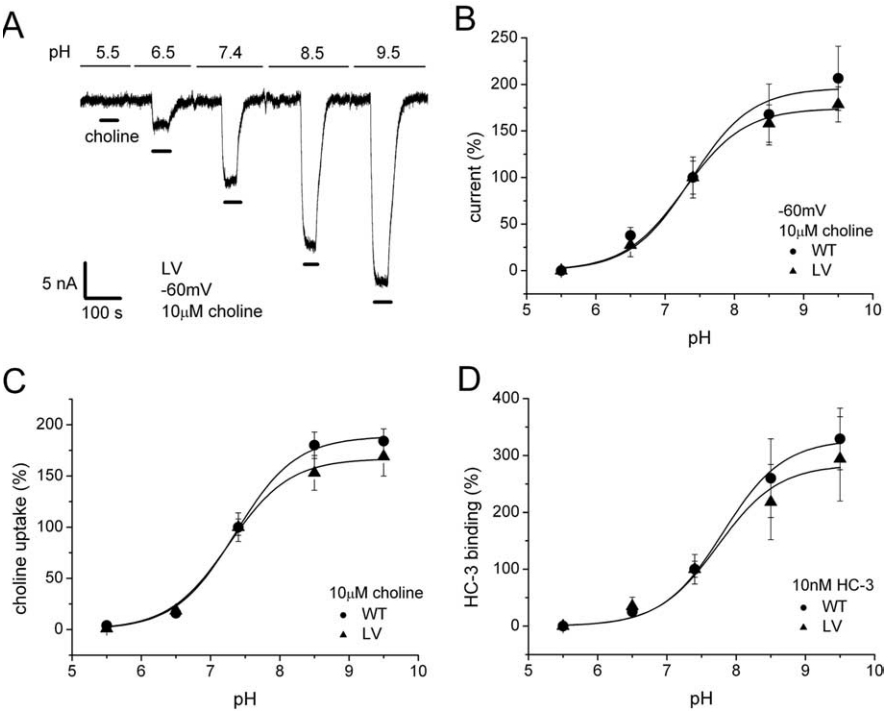

Figure 7. pH dependence of choline-induced current, choline uptake, and HC-3 binding. ***A***, pH dependence of choline-induced current. Typical data are shown for 10 μM choline-induced current for LV at −60 mV in 100 mM NaCl buffer. The slow baseline drift is removed from the figure. ***B***, pH dependence of 10 μM choline-induced currents at −60 mV are measured for WT and LV ($n = 5$). The data were normalized to pH 7.4 and fitted to a single-binding-site model. pKa of 7.4 ± 0.1 and I_{max} of 196.3 ± 10.5% for WT. pKa of 7.3 ± 0.1 and I_{max} of 174.4 ± 4.0% for LV. ***C***, pH dependence of choline uptake was measured in 10 μM choline (1% [^{3}H]choline) for 30 min ($n = 8$). pKa of 7.4 ± 0.1 and V_{max} of 188.8 ± 3.7% for WT. pKa of 7.3 ± 0.1 and V_{max} of 167.0 ± 3.8% for LV. ***D***, pH dependence of HC-3-specific binding was measured in 10 nM [^{3}H]HC-3 for 30 min ($n = 6–8$). pKa of 7.8 ± 0.1 and maximum binding (B_{max}) of 328.0 ± 10.0% for WT. pKa of 7.7 ± 0.2 and B_{max} of 283.6 ± 17.8% for LV.

Discussion

Choline transport is electrogenic with variable stoichiometry

From this study, choline transport is a voltage-dependent, electrogenic process with variable charge/choline stoichiometry (10 at −80 mV and 3 at −20 mV). Other members of the SLC5 family to which CHT belongs exhibit tight coupling and fixed stoichiometry, e.g., two Na^+ ions per substrate molecule (Eskandari et al., 1997; Loo et al., 2000; Prasad and Ganapathy, 2000; Diez-Sampedro et al., 2001; Wright et al., 2004). However, hSGLT3, also a member of the SLC5 family, is described as a glucose-gated ion channel (Diez-Sampedro et al., 2003), suggesting functional diversity of the SLC5 family (Wright et al., 2004). Whether the extra charge contributes to coupled transport is unknown, and slippage occurs alongside choline transport, as has been generally proposed for a host of transporters (Nelson et al., 2002). Na^+-coupled transport with variable stoichiometry that may depend on voltage is found in neurotransmitter transporters such as SERT (Mager et al., 1994; Galli et al., 1997), NET (Galli et al., 1998), dopamine transporter (DAT) (Sonders et al., 1997; Kahlig et al., 2005), and glutamate transporters (Wadiche et al., 1995).

The LV mutant increases surface expression without altering WT properties

Stable hCHT WT expression is low in mammalian cells because hCHT is efficiently endocytosed from the plasma membrane (Ferguson and Blakely, 2004; Ribeiro et al., 2005). Low plasma membrane levels of hCHT are known to impede reliable measurements such as transport assays (Apparsundaram et al., 2000) and freeze-fracture electron microscopic studies (Wright and Turk, 2004). Whole-oocyte choline-induced currents under physiological conditions (100 mM NaCl, pH 7.4) yield ~5 nA at −60 mV, which is close to our detection limit (1 nA) and primarily restrict our studies. However, a trafficking mutant LV that slows down internalization effectively increased hCHT on the surface by approximately threefold, which greatly improve accuracy of our measurements. To assess whether changes occur other than trafficking, we compared transport and electrophysiology in hCHT WT and LV. In oocytes, the LV mutant increases surface expression with almost no change in intrinsic hCHT properties, consistent with mammalian cell data and suggesting that frog oocytes constitutively internalize hCHT via di-leucine trafficking motifs in the C terminal (Ribeiro et al., 2005) (Ruggiero, Ferguson, and Blakely, unpublished observation). The LV mutant has similar choline affinity (Fig. 3*C*), HC-3 sensitivity (Fig. 4*C*,

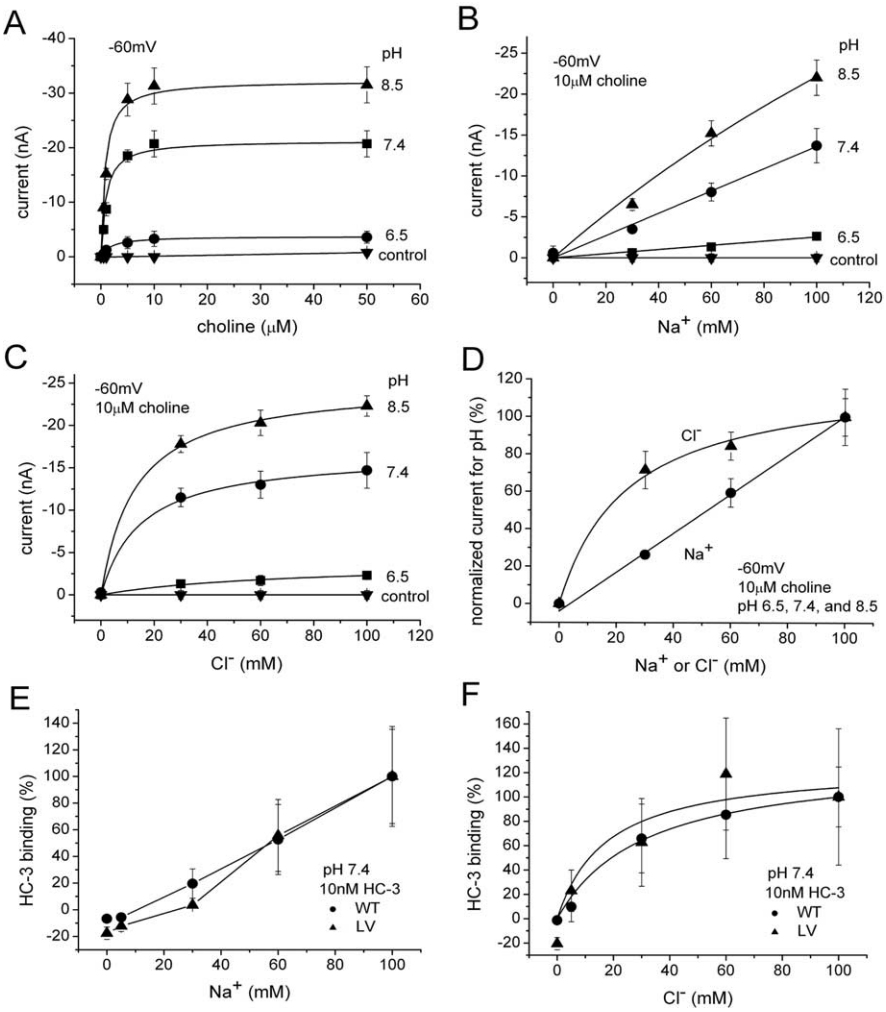

Figure 8. Effect of pH on K_m and I_{max}. ***A***, K_m and I_{max} for choline-induced currents measured at different pH and held at −60 mV ($n = 3$). At pH 6.5, K_m of 1.9 ± 0.3 μM and I_{max} of −3.8 ± 0.1 nA. At pH 7.4, K_m of 0.9 ± 0.3 μM and I_{max} of −21.3 ± 0.4 nA. At pH 8.5, K_m of 0.8 ± 0.2 μM and I_{max} of −32.3 ± 0.5 nA. LV-expressing oocytes were used. As a control, three water-injected oocytes were measured at each pH 6.5, 7.4, and 8.5. ***B***, Na^+ dependence of choline-induced current at various pH. In 10 μM choline, the induced current was measured at −60 mV, because LiCl replaced NaCl at different pH ($n = 3$). The Na dependence is linear at all pH. LV-expressing oocytes were used. ***C***, Cl^- dependence of choline-induced current at various pH ($n = 3$). In 10 μM choline, the induced current at −60 mV is measured at different pH (Na gluconate replacing NaCl). Results at 6.5 were insufficiently precise, although saturation clearly occurs. K_m of 67.2 ± 22.5 mM and I_{max} of −3.8 ± 0.6 nA for pH 6.5. K_m of 14.9 ± 3.4 mM and I_{max} of −16.7 ± 0.7 nA for pH 7.4. K_m of 12.8 ± 1.7 mM and I_{max} of −25.0 ± 0.5 nA for pH 8.5. LV-expressing oocytes were used. ***D***, Na^+ and Cl^- dependence of the choline-induced current do not depend on pH. Data from ***B*** and ***C*** are normalized for all pH and averaged. For Cl^-, K_m of 23.6 ± 5.8 mM and I_{max} of 122.2 ± 7.6%. ***E***, Na^+ dependence of HC-3 binding ($n = 6–8$). Na^+ dependence of HC-3 binding is similar to that of choline-induced current (***D***). ***F***, Cl^- dependence of HC-3 binding ($n = 6–8$). Cl^- dependence of HC-3 binding is similar to that of choline-induced current (***D***). Cl^- dependence is fitted to a single-binding-site model. K_m of 31.2 ± 3.8 mM and B_{max} of 131.0 ± 4.8% for WT. K_m of 17.5 ± 20.4 mM and B_{max} of 126.4 ± 30.7% for LV.

8*E*,*F*), ion dependence (Fig. 5*D*), and pH dependence (Fig. 7*B–D*). Transport and current are also similar, except they are approximately three times larger in the mutant. The LV reversal potential may indicate a slight difference in ion selectivity compared with WT (Figs. 1*B*, 3*A*,*B*), but this apparent difference could result from improved accuracy attributable to larger LV currents.

Constitutive leak currents through hCHT depolarize oocytes

The selective blocker HC-3 reveals a leak current through hCHT in the absence of choline. Simultaneous measurement of [$^{22}Na^+$] uptake and current demonstrated that leak currents in the related carrier rabbit SGLT1 are carried by Na^+ ions (Mackenzie et al., 1998). Other transporters, such as SERT (Mager et al., 1994; Galli et al., 1997; Petersen and DeFelice, 1999), NET (Galli et al., 1995), DAT (Sonders et al., 1997), and SGLT1 (Hirayama et al., 1994) also exhibit leak currents in the absence of substrates. Resting potentials in hCHT-expressing oocytes, but in the absence of choline, are depolarized by 20–30 mV compared with water-injected control oocytes. This constitutive depolarization was reduced by ~50% when oocytes were preincubated with 1 μM HC-3 for a few days before experimentation (data not shown). These data suggest the leak currents through hCHT are responsible for the depolarization. Furthermore, the depolarization in Figure 4*D* correlates with the holding current shift (Fig. 1*B*, inset) in hCHT-expressing versus control oocytes after ion substitution (Fig. 5*A–C*). In a neuronal environment, the constitutive depolarizing leak could have important consequences for voltage-sensitive channels and nerve terminal excitability.

Cl^- plays a regulatory role in choline transport

The reversal potential (45–60 mV, depending on choline concentration) (Figs. 1*B*, 3*B*) suggests that choline-induced current is Na^+ selective; the Nernst potential for Na^+ is 40 mV, assuming external Na^+ of 100 mM and internal Na^+ of 22 mM in oocytes (Kusano et al., 1982). However, the ion substitutions indicate that both external Na^+ and Cl^- are required for the choline-induced current (Fig. 5*D*) and choline uptake (Simon and Kuhar, 1976; Kuhar and Murrin, 1978; Okuda and Haga, 2000). Interestingly, CHT is the only member of the SLC5 family that displays strict Cl^- requirement (composed of 11 members in human) (Wright and Turk, 2004). Although SGLT1 has moderate Cl^- sensitivity, Loo et al. (2000) show that no Cl^- is cotransported with substrate. In addition, Na^+ and Cl^- dependencies have strikingly different ionic dependences under voltage clamp (Fig. 8*B*,*C*): Na^+ titration shows almost linear dependence (Fig. 8*B*), similar to channel conductance, whereas Cl^- titration exhibits saturation, which is suggestive of binding (Fig. 8*C*). These data suggest that Cl^- may play a role as a requisite regulator rather than a cotransported ion. In support of this theory, choline-induced current is sensitive to internal Na^+ but insensitive to internal Cl^- (Fig. 6*A*,*B*), similar to previous studies in hSERT using the cut-open oocyte voltage-clamp technique (Adams and DeFelice, 2003). However, a 5-HT-gated influx of Cl^- has been measured in rSERT (Quick, 2003), and a similar Cl^- flux is observed in DAT (Ingram et al., 2002; Carvelli et al., 2004). Additional investigations are

necessary to establish a clear role of Cl^- for Na^+-coupled transporters in general.

Possible pH regulation mechanism

Neurotransmitter transporter pH dependence is well studied in rSERT (Cao et al., 1997, 1998), which is activated at low pH, opposite to our finding for hCHT. The Na^+–glucose cotransporter SGLT1 is also activated at low pH, and, in this case, H^+ can actually replace Na^+ as the driving co-ion for glucose transport (Hirayama et al., 1994). Because hCHT belongs to the same gene family as SGLT1, similar pH effects might have been expected. hCHT transport and induced current are, however, inactivated at low pH and enhanced at high pH (Fig. 7*A*), revealing a sigmoidal pH dependence with pKa of 7.4 (Fig. 7*B*,*C*). A comparable pH effect has been reported in the glycine transporter subtype 1b, in which Na^+ and protons interact noncompetitively through different binding sites (Aubrey et al., 2000). HC-3-specific binding (Fig. 7*D*) exhibits similar pH dependence to hCHT current and uptake, possibly indicating that current, uptake, and binding are pH regulated by similar residues, although not necessarily at the same site. It is worth noticing that Sandberg and Coyle (1985) observed similar pH dependence of HC-3 binding in rat forebrain synaptosomal membranes. A pKa near 7 is characteristic of histidine residues in a hydrophobic environment (Aubrey et al., 2000; Keller and Parsons, 2000). In the choline transporter, five histidine residues exist, and four are presumably located on or near extracellular sites (Apparsundaram et al., 2000; Okuda and Haga, 2003). These histidine residues are suspected to be the sites of proton interaction and regulation and are targets for mutations and subsequent analysis, now under investigation.

Proton inactivation hypothesis of hCHT in synaptic vesicles

Recent immunogold staining data (Ferguson et al., 2003; Nakata et al., 2004) revealed that the majority of CHT (70–90%) are located on presynaptic vesicles rather than the plasma membrane. In the synaptic vesicles, pH is low via the action of vesicular ATPase; the vesicle lumen has pH 5.5, whereas cytoplasmic pH is typically 7.5 (Eiden, 1998). In cholinergic neurons, VAChT uses this large H^+ gradient to counter-transport acetylcholine from the cytoplasm into the synaptic vesicles. Any proton leakage through hCHT would be detrimental to the driving force that concentrates vesicular ACh 100 times over cytoplasmic ACh [~100 over 1 mM, respectively (Parsons et al., 1993; Nguyen et al., 1998)]. Furthermore, at high ACh concentrations, it has been suggested that ACh can permeate choline transporters (Marchbanks and Wonnacott, 1979), possibly because H^+ replaces Na^+ as a cotransported ion, similar to SGLT1 (Hirayama et al., 1994). We observed an ACh-induced current in hCHT-expressing oocytes but not control oocytes (data not shown); however, because ACh is easily degraded, we cannot exclude the possibility of free choline in ACh applications. Although it appears likely that ACh permeates hCHT and that low pH inhibits this permeation, this aspect of our hypothesis needs additional testing.

Because vesicles deliver CHTs to the plasma membrane according to need, the question arises whether they are functional in the vesicle; in particular, are CHTs barred from leaking ACh and possibly protons from this compartment. Acidic inactivation of CHTs may provide the mechanism that prevents such leakage from synaptic vesicles in cholinergic neurons. The distribution of transporters on synaptic vesicles has also been observed for glycine transporters (Geerlings et al., 2001) and L-proline transporters (Renick et al., 1999), suggesting that evolution of a tight pH regulation system to allow use of the vesicles to support activity-dependent trafficking (Ferguson et al., 2003).

References

Adams SV, DeFelice LJ (2003) Ionic currents in the human serotonin transporter reveal inconsistencies in the alternating access hypothesis. Biophys J 85:1548–1559.

Apparsundaram S, Ferguson SM, George Jr AL, Blakely RD (2000) Molecular cloning of a human, hemicholinium-3-sensitive choline transporter. Biochem Biophys Res Commun 276:862–867.

Apparsundaram S, Ferguson SM, Blakely RD (2001) Molecular cloning and characterization of a murine hemicholinium-3-sensitive choline transporter. Biochem Soc Trans 29:711–716.

Aubrey KR, Mitrovic AD, Vandenberg RJ (2000) Molecular basis for proton regulation of glycine transport by glycine transporter subtype 1b. Mol Pharmacol 58:129–135.

Bales KR, Tzavara ET, Wu S, Wade MR, Bymaster FP, Paul SM, Nomikos GG (2006) Cholinergic dysfunction in a mouse model of Alzheimer disease is reversed by an anti-Aβ antibody. J Clin Invest 116:825–832.

Bymaster FP, McKinzie DL, Felder CC, Wess J (2003) Use of M_1-M_5 muscarinic receptor knockout mice as novel tools to delineate the physiological roles of the muscarinic cholinergic system. Neurochem Res 28:437–442.

Cao Y, Mager S, Lester HA (1997) H^+ permeation and pH regulation at a mammalian serotonin transporter. J Neurosci 17:2257–2266.

Cao Y, Li M, Mager S, Lester HA (1998) Amino acid residues that control pH modulation of transport-associated current in mammalian serotonin transporters. J Neurosci 18:7739–7749.

Carvelli L, McDonald PW, Blakely RD, DeFelice LJ (2004) Dopamine transporters depolarize neurons by a channel mechanism. Proc Natl Acad Sci USA 101:16046–16051.

Collier B, Kwok YN, Welner SA (1983) Increased acetylcholine synthesis and release following presynaptic activity in a sympathetic ganglion. J Neurochem 40:91–98.

Dani JA, DeBiasi M (2001) Cellular mechanisms of nicotine addiction. Pharmacol Biochem Behav 70:439–446.

Diez-Sampedro A, Eskandari S, Wright EM, Hirayama BA (2001) Na^+-to-sugar stoichiometry of SGLT3. Am J Physiol Renal Physiol 49:F278–F282.

Diez-Sampedro A, Hirayama BA, Osswald C, Gorboulev V, Baumgarten K, Volk C, Wright EM, Koepsell H (2003) A glucose sensor hiding in a family of transporters. Proc Natl Acad Sci USA 20:11753–11758.

Eiden LE (1998) The cholinergic gene locus. J Neurochem 70:2227–2240.

Eskandari S, Loo DDF, Dai G, Levy O, Wright EM, Carrasco N (1997) Thyroid Na^+/I^- symporter: mechanism, stoichiometry, and specificity. J Biol Chem 272:27230–27238.

Ferguson SM, Blakely RD (2004) The choline transporter resurfaces: new roles for synaptic vesicles? Mol Intervent 4:22–37.

Ferguson SM, Savchenko V, Apparsundaram S, Zwick M, Wright J, Heilman CJ, Yi H, Levey AI, Blakely RD (2003) Vesicular localization and activity-dependent trafficking of presynaptic choline transporters. J Neurosci 23:9697–9709.

Ferguson SM, Bazalakova M, Savchenko V, Tapia JC, Wright J, Blakely RD (2004) Lethal impairment of cholinergic neurotransmission in hemicholinium-3-sensitive choline transporter knockout mice. Proc Natl Acad Sci USA 101:8762–8767.

Galli A, DeFelice LJ, Duke BJ, Moore KR, Blakely RD (1995) Sodium-dependent norepinephrine-induced currents in norephinephrine-transporter-transfected HEK-293 cells blocked by cocaine and antidepressants. J Exp Biol 198:2197–2212.

Galli A, Petersen CI, deBlaquiere M, Blakely RD, DeFelice LJ (1997) *Drosophila* serotonin transporters have voltage-dependent uptake coupled to a serotonin-gated ion channel. J Neurosci 17:3401–3411.

Galli A, Blakely RD, DeFelice LJ (1998) Patch-clamp and amperometric recordings from norepinephrine transporters: channel activity and voltage-dependent uptake. Proc Natl Acad Sci USA 95:13260–13265.

Geerlings A, Nunez E, Lopez-Corcuera B, Aragon C (2001) Calcium- and syntaxin 1-mediated trafficking of the neuronal glycine transporter GLYT2. J Biol Chem 276:17584–17590.

Guyenet P, Lefresne P, Rossier J, Beaujouan JC, Glowinski J (1973) Inhibition by hemicholinium-3 of [^{14}C]acetylcholine synthesis and [^{3}H]choline high-affinity uptake in rat striatal synaptosomes. Mol Pharmacol 9:630–639.

Haga T, Noda H (1973) Choline uptake systems of rat brain synaptosomes. Biochim Biophys Acta 291:564–575.

Hirayama BA, Loo DDF, Wright EM (1994) Protons drive sugar transport through the Na^+/glucose cotransporter (SGLT1). J Biol Chem 269:21407–21410.

Ingram SL, Prasad BM, Amara SG (2002) Dopamine transporter-mediated conductances increase excitability of midbrain dopamine neurons. Nat Neurosci 5:971–978.

Kahlig KM, Binda F, Khoshbouei H, Blakely RD, McMahon DG, Javitch JA, Galli A (2005) Amphetamine induces dopamine efflux through a dopamine transporter channel. Proc Natl Acad Sci USA 102:3495–3500.

Karakossian MH, Spencer SR, Gomez AQ, Padilla OR, Sacher A, Loo DDF, Nerson N, Eskandari S (2005) Novel properties of a mouse γ-aminobutyric acid transporter (GAT4). J Membr Biol 203:65–82.

Keller JE, Parsons SM (2000) A critical histidine in the vesicular acetylcholine transporter. Neurochem Int 36:113–117.

Kuhar MJ, Murrin LC (1978) Sodium-dependent, high affinity choline uptake. J Neurochem 30:15–21.

Kusano K, Miledi R, Sinnakre J (1982) Cholinergic and catecholaminergic receptors in the *Xenopus* oocyte membrane. J Physiol (Lond) 328:143–170.

Loo DDF, Eskandari S, Boorer KJ, Sarkar HK, Wright EM (2000) Role of Cl^- in electrogenic Na^+-coupled cotransporters GAT1 and SGLT1. J Biol Chem 275:37414–37422.

Lowenstein PR, Coyle JT (1986) Rapid regulation of [^{3}H]hemicholinium-3 binding sites in the rat brain. Brain Res 381:191–194.

Mackenzie B, Loo DDF, Wright EM (1998) Relationships between Na^+/glucose cotransporter (SGLT1) currents and fluxes. J Membr Biol 162:101–106.

Mager S, Min C, Henry DJ, Chavkin C, Hoffman BJ, Davidson N, Lester HA (1994) Conducting states of a mammalian serotonin transporter. Neuron 12:845–859.

Mager S, Kleinberger-Doron N, Keshet GI, Davidson N, Kanner BI, Lester HA (1996) Ion binding and permeation at the GABA transporter GAT1. J Neurosci 16:5405–5414.

Marchbanks RM, Wonnacott S (1979) Relationship of choline uptake to acetylcholine synthesis and release. Prog Brain Res 49:77–88.

Ming L, Farley RA, Lester HA (2002) Voltage-dependent transient currents of human and rat 5-HT transporters (SERT) are blocked by HEPES and ion channel ligands. FEBS Lett 513:247–252.

Nakata K, Okuda T, Misawa H (2004) Ultrastructural localization of high-affinity choline transporter in the rat neuromuscular junction: enrichment on synaptic vesicles. Synapse 53:53–56.

Nelson N, Sacher A, Nelson H (2002) The significance of molecular slips in transport systems. Nat Rev Mol Cell Biol 3:876–881.

Nguyen ML, Cox GD, Parsons SM (1998) Kinetic parameters for the vesicular acetylcholine transporter: two protons are exchanged for one acetylcholine. Biochemistry 37:13400–13410.

Okuda T, Haga T (2000) Functional characterization of the human high-affinity choline transporter. FEBS Lett 484:92–97.

Okuda T, Haga T (2003) High-affinity choline transporter. Neurochem Res 28:483–488.

Okuda T, Haga T, Kanai Y, Endou H, Ishihara T, Katsura I (2000) Identification and characterization of the high-affinity choline transporter. Nat Neurosci 3:120–125.

Parsons SM, Prior C, Marshall IG (1993) Acetylcholine transport, storage, and release. Int Rev Neurobiol 35:279–390.

Perrin DD (1972) Dissociation constants of organic bases in aqueous solution. London: Butterworths.

Petersen CI, DeFelice LJ (1999) Ionic interactions in the *Drosophila* serotonin transporter identify it as a serotonin channel. Nat Neurosci 2:605–610.

Prasad PD, Ganapathy V (2000) Structure and function of mammalian sodium-dependent multivitamin transporter. Curr Opin Clin Nutr Metab Care 3:263–266.

Quick MW (2003) Regulating the conducting states of a mammalian serotonin transporter. Neuron 40:537–549.

Ramsey IS, DeFelice LJ (2002) Serotonin transporter function and pharmacology are sensitive to expression level: evidence for an endogenous regulatory factor. J Biol Chem 277:14475–14482.

Renick SE, Kleven DT, Chan J, Stenius K, Milner TA, Pickel VM, Fremeau Jr RT (1999) The mammalian brain high-affinity L-proline transporter is enriched preferentially in synaptic vesicles in a subpopulation of excitatory nerve terminals in rat forebrain. J Neurosci 19:21–33.

Ribeiro FM, Black SAG, Cregan SP, Prado VF, Prado MAM, Rylett RJ, Ferguson SSG (2005) Constitutive high-affinity choline transporter endocytosis is determined by a carboxyl-terminal tail dileucine motif. J Neurochem 94:86–96.

Ribeiro FM, Black SAG, Prado VF, Rylett RJ, Ferguson SSG, Prado MAM (2006) The "ins" and "outs" of the high-affinity choline transporter CHT1. J Neurochem 97:1–12.

Sandberg K, Coyle J (1985) Characterization of [^{3}H]hemicholinium-3 binding associated with neuronal choline uptake sites in rat brain membranes. Brain Res 348:321–330.

Sarter M, Parikh V (2005) Choline transporters, cholinergic transmission and cognition. Nat Neurosci 6:48–56.

Simon JR, Kuhar MJ (1975) Impulse-flow regulation of high affinity choline uptake in brain cholinergic nerve terminals. Nature 255:162–163.

Simon JR, Kuhar MJ (1976) High affinity choline uptake: ionic and energy requirements. J Neurochem 27:93–99.

Sonders MS, Zhu S, Zahniser NR, Kavanaugh MP, Amara SG (1997) Multiple ionic conductances of the human dopamine transporter: the actions of dopamine and psychostimulants. J Neurosci 17:960–974.

Tan PK, Waites C, Liu Y, Krantz DE, Edwards RH (1998) A leucine-based motif mediates the endocytosis of vesicular monoamine and acetylcholine transporters. J Biol Chem 273:17351–17360.

Wadiche JI, Amara SG, Kavanaugh MP (1995) Ion fluxes associated with excitatory amino acid transport. Neuron 15:721–728.

Wright EM, Turk E (2004) The sodium/glucose cotransport family SLC5. Pflügers Arch 447:510–518.

Wright EM, Loo DDF, Hirayama BA, Turk E (2004) Surprising versatility of Na^+-glucose cotransporters: SLC5. Physiology (Bethesda) 19:370–376.

Yamamura HI, Snyder SH (1972) Choline: high-affinity uptake by rat brain synaptosomes. Science 178:626–628.